Original article

Polysubstituted pyrazoles, part 5.[1] Synthesis of new 1-(4-chlorophenyl)-4-hydroxy-1*H*-pyrazole-3-carboxylic acid hydrazide analogs and some derived ring systems. A novel class of potential antitumor and anti-HCV agents☆

Sherif A.F. Rostom [a,*], Manal A. Shalaby [b], Maha A. El-Demellawy [b]

[a] *Department of Medicinal Chemistry, Faculty of Medicine and Allied Sciences, King Abdul-Aziz University, P.O. Box 80205, Jeddah 21589, Saudi Arabia*

[b] *Genetic Engineering and Biotechnology Research Institute (GEBRI), Mubarak City for Scientific Research and Technology Applications, Bourg El-Arab, Alexandria, Egypt*

Abstract

A novel series of 1-(4-chlorophenyl)-4-hydroxy-1*H*-pyrazole-3-carboxylic acid hydrazide analogs and some derived 4-substituted-1,2,4-triazolin-3-thiones, 2-substituted-1,3,4-thiadiazole and 2-substituted-1,3,4-oxadiazoles has been synthesized. Ten of the newly synthesized compounds were selected by the National Cancer Institute (NCI)-in vitro-disease oriented antitumor screening to be evaluated for their antitumor activity. Seven compounds, namely **7a–c**, **9**, **11**, **13** and **14**, exhibited potential and broad spectrum antitumor activity against most of the tested subpanel tumour cell lines ($GI_{50} < 100$ μM). Compounds **14** (GI_{50}, TGI, and LC_{50} MG-MID values of 0.08, 15.8 and 64.6 μM, respectively) and **11** (GI_{50}, TGI, and LC_{50} MG-MID values of 0.20, 11.7 and 87.1 μM, respectively) proved to be the most active members in this study with potential activity against all the tested subpanel tumour cell lines and particular effectiveness on the leukaemia subpanel at both the GI_{50} (0.03 and 0.09 μM, respectively) and the TGI levels (35.2 and 28.1 μM, respectively). Moreover, compound **14** exhibited a super sensitivity profile towards about 26 different cancer cell lines with GI_{50} values lying in the nanomolar concentration range (GI_{50} values < 0.01 μM). In addition, compounds **2–5**, **6a–d**, **7a**, **8–11**, **12a**, **13**, **14** were investigated for their in vitro effect on the replication of hepatitis-C virus (HCV) in HepG2 hepatocellular carcinoma cell line infected with the virus using the reverse transcription–polymerase chain reaction (RT-PCR) technique. The results revealed that compounds **2** and **5** were capable of inhibiting the replication of both the HCV RNA (+) and (−) strands at 10–100 μg mL^{-1} concentration range.
© 2003 Éditions scientifiques et médicales Elsevier SAS. All rights reserved.

Keywords: 1*H*-pyrazoles; acid hydrazide derivatives; 1,2,4-triazolin-3-thiones; 1,3,4-thiadiazole; 1,3,4-oxadiazoles; antitumor activity; anti-HCV activity; RT-PCR

1. Introduction

Identification of novel structure leads that may be of use in designing new, potent, selective and less toxic anticancer agents remains a major challenge for medicinal chemistry researchers. In this view, the discovery of the natural 4-hydroxypyrazole C-glycoside antibiotic Pyrazofurin; 4-hydroxy-3β-D-ribofuranosyl-1*H*-pyrazole-5-carboxamide (Fig. 1); has provided a basis for more rationale design and synthesis of new pyrazoles as potential antimicrobial [1–3], antiviral [4–6] and anticancer agents [7–9]. Pyrazofurin; isolated from *Streptomyces candidus*; bears a clear structure resemblance to ribaverin; 1β-D-ribofuranosyl-1*H*-1,2,4-triazole-3-carboxamide (Fig. 1) and other five-membered nucleosides but unlike those, it inhibits the de novo synthesis of pyrimidines rather than the structurally related purines.

---

* Corresponding author.

E-mail address: sherifrostom@yahoo.com (Sh.A.F. Rostom).

[1] For part 4: see Ref. [18].
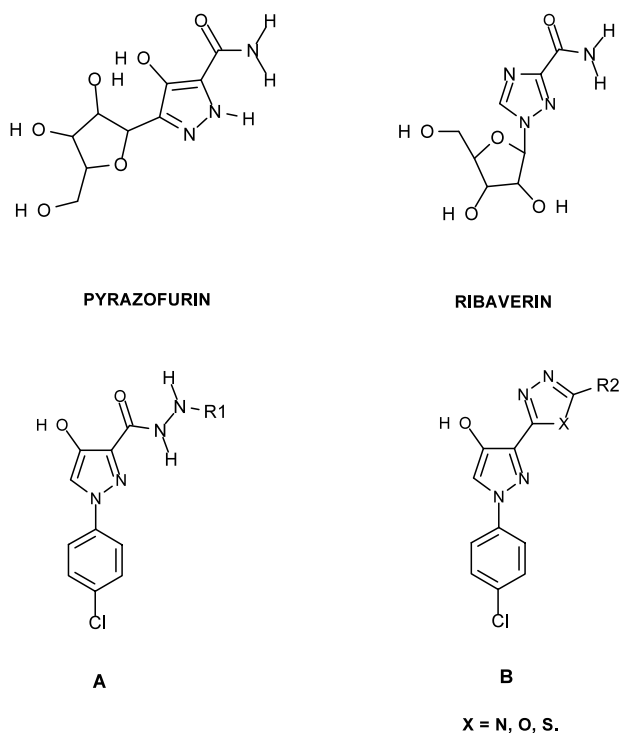
PYRAZOFURIN

RIBAVERIN

A

B

X = N, O, S.

Fig. 1.

This antibiotic was believed to act as an antagonist of uridine metabolism and the monophosphate inhibits the OMP decarboxylase enzyme [10]. Pyrazofurin has received considerable attention as a result of its various biological effects including the potent antimicrobial and broad-spectrum antiviral activities against many RNA and DNA viruses. As has been also noted, pyrazofurin has been evaluated against several tumour cell lines, consequently, it has only been used clinically as an anticancer agent. Although pyrazofurin and its analogs will continue to be pursued for their chemotherapeutic value, the critical hurdle still to be overcome is the unavailability and inherent toxicity of the drug [11].

On the other hand, over the past decade, there has been growing interest in acute and chronic liver diseases that are caused by an infection with hepatitis-C virus (HCV), such as hepatocellular carcinoma and liver cirrhosis. It has been recently reported that about 3% of the world population is infected with this harmful pathogen that can cause a variety of complicated clinical symptoms, 90–95% of which through blood transfusion and haemodialysis [12]. HCV is a small-enveloped virus belonging to the Flaviviridea with single-stranded RNA genome that codes for a single polyprotein [13]. Recently, HCV is believed to act as a carcinogen by virtue of the increased risk of hepatocellular carcinoma among persistently infected patients with chronic active hepatitis. This was attributed to the fact that HCV causes an immune-mediated chronic inflammation in the liver with the resulting cell damage eventually giving rise to

transformation and hepatocellular carcinoma [14]. Moreover, some clinical studies indicated a significant correlation between HCV infection and some lymphoproliferative disorders, especially the high prevalence of auto-antibodies, mixed cryoglobulinemia and non-Hodgkin lymphoma, suggesting that HCV not only causes a liver disease but rather a multifaceted clinical syndrome [15]. The inherent instability of this virus gave rise to multiple types and subtypes which have seriously hampered efforts to develop an efficient HCV vaccine [16]. As yet, the only available therapy for chronic HCV infection is the treatment with interferon-alpha (Ifn-α) either alone or in combination with the nucleoside analog ribaverin. Unfortunately, only 40% of treated patients develop a sustained response that is defined by the absence of viral RNA for more than 6 months after cessation of the therapy. In spite of the beneficial effect of rebaverin, the side effects are intensified with combination therapy as it can cause severe haemolytic anaemia in addition to its possible teratogenic effect [15,17]. These complications clearly document the need for more effective, less toxic anticancer and antiviral therapies.

In view of the above-mentioned findings, and in continuation of our interest in biologically active pyrazoles [18–22], the aim of the present study was to synthesize and investigate the in vitro anticancer activity of some novel 4-hydroxy-1*H*-pyrazole-3-carboxylic acid hydrazide analogs **A** carrying the vicinal hydroxyl and amidic pharmacophores of pyrazofurin, in addition to some derived ring systems having the general formula **B** (Fig. 1). It was also considered of interest to confirm the ability of the newly synthesized compounds to inhibit the replication of the HCV RNA (as a possible carcinogen) by a reliable and reproducible biotechnological technique; the RT-PCR. Careful literature survey for functional groups which could be considered as pharmacophores for the anticancer and antiviral activities revealed that the amide function is common among most of the natural antibiotic antitumor and antiviral agents such as bleomycin, netropsin and pyrazofurin [23]. Therefore, the target compounds were rationalized so as to comprise the amidic pharmacophores that are believed to be responsible for the biological significance of some relevant chemotherapeutic agents, such as the *N*-formyl, *N*-acetyl, semicarbazide, thiosemicarbazide and azomethine functionalities [24–29]. The substitution pattern of such amide derivatives was carefully selected so as to confer different electronic environment to the molecules. Based on the fact that substituted 1,2,4-triazoles and 1,3,4-thiadiazoles have been contributed to a variety of chemotherapeutic activities [30–33], it was planned to synthesize hybrid compounds that comprise both the 4-hydroxypyrazole and the aforementioned heterocyclic ring systems. Such hybridization was designed in an attempt to obtain synergistic chemother-

apeutic activity with higher selectivity and less toxicity. Moreover, owing to the increasing biological importance of 1,3,4-oxadiazoles, particularly in the field of chemotherapy [34–36], it was considered of interest to link the 4-hydroxypyrazole backbone to some 1,3,4-oxadiazoles and their 1,3,4-oxadiazoline-5-thione, 1,3,4-oxadiazoline-5-one analogs in order to investigate the effect of such structure variation on the anticipated antitumor and/or antiviral activities.

2. Chemistry

The synthetic strategies adopted to obtain the target compounds are depicted in Figs. 2 and 3. The key intermediate in the present study is the 1-(4-chlorophenyl)-4-hydroxy-1*H*-pyrazole-3-carboxylic acid hydrazide **1**, which was prepared according to a previously described procedure [18]. When **1** was refluxed with formic acid, the target *N*-formyl-1-(4-chlorophenyl)-4-hydroxy-1*H*-pyrazole-3-carboxylic acid hydrazide **2** was obtained in a good yield. Warming **1** with acetic anhydride afforded the *N*-acetyl-4-acetyloxy-1-(4-chlorophenyl)-1*H*-pyrazole-3-carboxylic acid hydrazide **3**. Reacting the same starting compound **1** with phenyl isocyanate or a variety of isothiocyanates resulted in the

formation of the corresponding 4-phenyl-1-(1-(4-chlorophenyl)-4-hydroxy-1*H*-pyrazole-3-carbonyl)semi-carbazide **4** and the 4-substituted thiosemicarbazides **6a**–**d**, respectively. On the other hand, heating **1** with ammonium thiocyanate in the presence of dilute hydrochloric acid afforded the 1-(1-(4-chlorophenyl)-4-hydroxy-1*H*-pyrazole-3-carbonyl)thiosemicarbazide **5** in a moderate yield. Alkaline cyclisation of the 4-substituted thiosemicarbazides **6a**–**c** using sodium hydroxide afforded the corresponding 5-(1-(4-chlorophenyl)-4-hydroxy-1*H*-pyrazol-3-yl)-4-substituted-1,2,4-triazolin-3-thiones **7a**–**c** in excellent yields. Furthermore, reacting the thiosemicarbazide **6a** with cold concentrated sulphuric acid resulted in the formation of the corresponding 5-(1-(4-chlorophenyl)-4-hydroxy-1*H*-pyrazol-3-yl)-2-phenylamino-1,3,4-thiadiazole **8**. Cyclisation of **6a** to 5-(1-(4-chlorophenyl)-4-hydroxy-1*H*-pyrazol-3-yl)-2-phenylamino-1,3,4-oxadiazole **9** could be achieved by boiling of the former with mercuric oxide in absolute ethanol (Fig. 2).

In Fig. 3, the preparation of the 5-(1-(4-chlorophenyl)-4-hydroxy-1*H*-pyrazol-3-yl)-1,3,4-oxadiazolin-2-thione **10** was achieved by adopting a simple one-pot procedure that involves reacting **1** with carbon disulfide under strong basic conditions followed by acidification with dilute hydrochloric acid. The synthesis of the 5-(1-
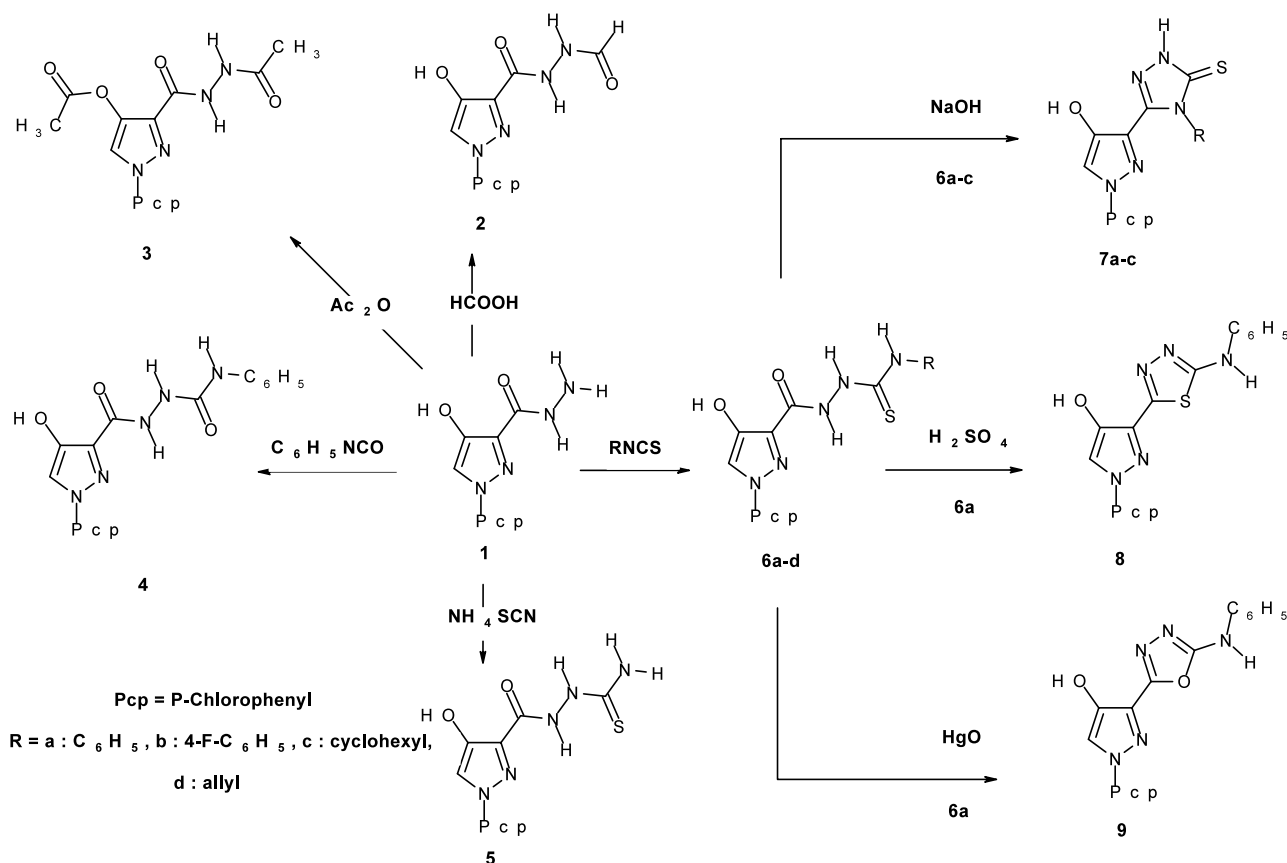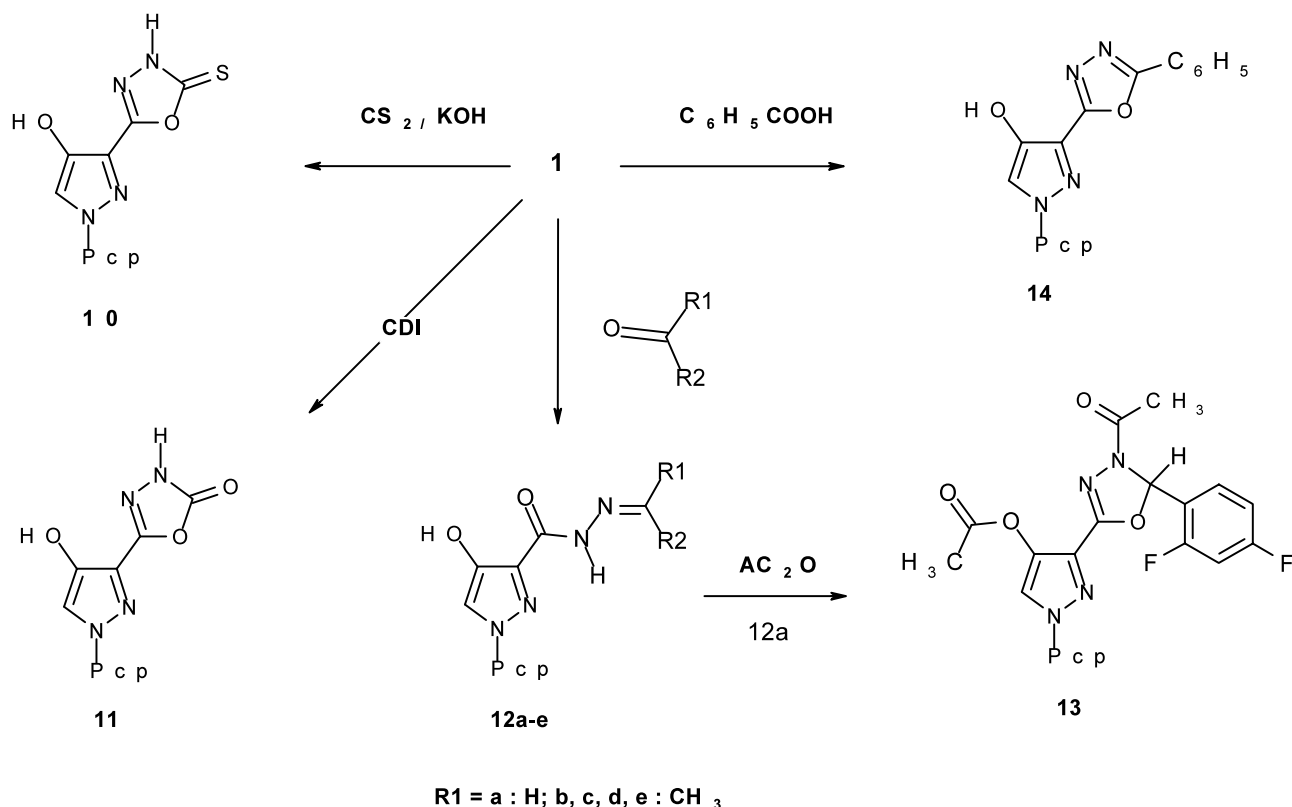

Fig. 2. Synthesis of compounds **2**–**9**.

Fig. 3. Synthesis of compounds **10–14**.

(4-chlorophenyl)-4-hydroxy-1*H*-pyrazol-3-yl)-1,3,4-oxa-diazolin-2-one **11** was accomplished by treating the key intermediate **1** with 1,1'-carbonyldiimidazole (CDI) in dry tetrahydrofuran (THF). Moreover, condensing the acid hydrazide **1** with a variety of aldehydes or ketones in acetic acid yielded the corresponding 3-(alkylidenehy-drazinocarbonyl)-1-(4-chlorophenyl)-4-hydroxy-1*H*-pyrazoles **12a**–**e**. Conversion of **12a** into the 3-acetyl-5-(4-acetyloxy-1-(4-chlorophenyl)-1*H*-pyrazol-3-yl)-2-(2,4-difluorophenyl)-1,3,4-oxadiazoline **13** was effected by treatment of the former compound with acetic anhydride. Finally, a convenient method for the synthesis of 5-(1-(4-chlorophenyl)-4-hydroxy-1*H*-pyrazol-3-yl)-2-phenyl-1,3,4-oxadiazole **14** was deduced from refluxing the acid hydrazide **1** with an equimolar amount of benzoic acid in the presence of an excess of phosphorus oxychloride (Fig. 3).

3. Results and discussion

3.1. In vitro antitumor screening

Out of newly synthesized pyrazole derivatives, compounds **3**, **7a**–**c**, **8**–**11**, **13** and **14** were selected by the National Cancer Institute (NCI) in vitro disease-or-iented human cells screening panel assay [37–39] to investigate their antitumor activities. About 60 cell lines of nine tumour subpanels, including leukaemia, non-small cell lung, colon, CNS, melanoma, ovarian, renal, prostate and breast cancer cell lines, were incubated with five concentrations (0.01–100 μM) for each compound and were used to create log concentration -% growth inhibition curves. Three response parameters (GI_{50}, TGI, and LC_{50}) were calculated for each cell line. The GI_{50} value (growth inhibitory activity) corresponds to the concentration of the compounds causing 50% decrease in net cell growth, the TGI value (cytostatic activity) is the concentration of the compounds resulting in total growth inhibition and the LC_{50} value (cytotoxic activity) is the concentration of the compounds causing net 50% loss of initial cells at the end of the incubation period (48 h). Subpanel and full panel mean-graph midpoint values (MG-MID) for certain agents are the average of individual real and default GI_{50}, TGI, or LC_{50} values of all cell lines in the subpanel or the full panel, respectively [37]. The NCI antitumor drug discovery was designed to distinguish between broad spectrum antitumor compounds and tumour or sub-panel-selective agents.

In the present study, only seven compounds, namely; the 5-(1-(4-chlorophenyl)-4-hydroxy-1*H*-pyrazol-3-yl)-

4-substituted-1,2,4-triazolin-3-thiones **7a**–**c** and the 5-(1-(4-chlorophenyl)-4-hydroxy-1*H*-pyrazol-3-yl)-2-substituted-1,3,4-oxadiazoles **9**, **11**, **13** and **14**, exhibited potential antitumor activities against most of the tested subpanel tumour cell lines (GI_{50}, TGI and LC_{50} values < 100 µM), whereas the other three compounds **3**, **8** and **10** proved to be totally inactive. Those seven compounds showed a distinctive potential pattern of sensitivity against some individual cell lines (Table 1), as

well as a broad spectrum of antitumor activity (Tables 2–4).

With regard to the sensitivity against some individual cell lines, compounds **7c**, **11** and **14** proved to be very sensitive towards most of the tested subpanel tumour cell lines with GI_{50} values range of < 0.01–0.66 µM. Compound **14** showed a super sensitivity profile towards about 26 different cancer cell lines with GI_{50} values lying in the nanomolar concentration range (GI_{50}

Table 1
Growth inhibitory concentration (GI_{50}, µM) of some selected in vitro tumour cell lines [a]

Cell lines	7a	7b	7c	9	10	13	14
Leukaemia							
HL-60(TB)	4.13	NT	NT [b]	NT	0.03	NT	< 0.01
K-562	3.95	12.6	< 0.01	NT	0.05	30.0	< 0.01
MOLT-4	62.7	14.7	0.63	NT	0.05	18.5	0.02
RPMI-8226	5.45	22.2	0.25	NT	0.12	20.5	0.09
SR	2.97	10.0	< 0.01	NT	NT	35.8	< 0.01
Non-small cell lung cancer							
A549/ATCC	14.1	13.2	0.93	20.4	0.18	33.2	< 0.01
HOP-62	9.92	22.7	0.47	17.7	0.20	28.8	< 0.01
NCI-H226	6.22	26.6	NT	8.39	0.27	NT	< 0.01
NCI-460	10.6	11.9	0.24	19.9	0.04	34.4	< 0.01
Colon cancer							
HCT-116	6.35	11.6	NT	16.1	0.09	33.4	< 0.01
HCT-15	3.36	11.3	0.15	10.4	0.30	32.2	< 0.01
HT29	19.8	43.2	39.1	9.56	2.02	40.1	0.25
KM12	4.35	13.0	0.39	17.8	0.12	25.4	< 0.01
CNS cancer							
SF-268	10.4	14.7	11.8	14.6	0.17	29.6	< 0.01
SF-295	4.95	14.8	< 0.01	18.9	NT	20.2	< 0.01
SF-539	5.91	15.1	NT	15.3	0.03	29.8	< 0.01
U251	10.8	15.8	NT	17.5	0.02	38.5	< 0.01
Melanoma							
MALME-3M	16.2	25.9	< 0.01	25.3	< 0.01	14.8	8.34
SK-MEL-5	4.19	14.3	0.23	11.4	0.36	18.4	< 0.01
UACC-257	20.7	24.2	0.87	21.3	0.43	27.2	0.51
UACC-62	11.4	12.0	< 0.01	16.5	0.28	28.8	0.23
Ovarian cancer							
OVCAR-3	2.51	22.0	< 0.01	31.9	NT	19.7	0.02
OVCAR-5	24.2	23.0	2.17	88.8	0.60	44.4	0.66
OVCAR-8	14.9	27.3	0.29	20.9	0.23	34.6	< 0.01
Renal cancer							
786-0	11.6	28.1	0.54	16.6	0.50	26.1	< 0.01
SN12C	17.8	16.9	0.84	16.1	0.31	33.6	< 0.01
TK-10	22.0	28.1	0.41	18.5	0.01	21.1	0.29
UO-31	14.2	25.0	13.5	14.3	0.23	31.9	< 0.01
Prostate cancer							
PC-3	27.5	14.8	10.0	NT	0.45	27.9	0.36
DU-145	22.3	22.0	0.33	15.4	0.05	39.2	0.31
Breast cancer							
MCF7	4.41	24.8	< 0.01	16.9	0.35	30.0	< 0.01
NCI/ADR-RES	3.79	15.4	< 0.01	14.9	0.18	42.9	0.03
HS 578T	7.64	29.1	0.3	24.1	0.08	31.8	< 0.01
MDA-MB-435	1.94	4.93	< 0.01	16.8	0.01	27.9	< 0.01

[a] Data obtained from NCI's in vitro disease-oriented human tumour cell screen.
[b] NT, not tested.

Table 2
Median growth inhibitory concentration (GI$_{50}$, μM) of in vitro subpanel tumour cell lines

Cpd. No.	Subpanel tumour cell lines [a]									MG-MID [b]
	I	II	III	IV	V	VI	VII	VIII	IX	
7a	15.8	22.9	10.3	11.7	14.1	19.3	14.7	24.9	15.8	11.0
7b	13.3	21.2	27.2	25.0	20.3	39.0	28.7	18.4	28.7	20.9
7c	0.23	9.60	31.7	4.11	4.17	11.3	19.3	5.16	14.2	0.65
9	NT [c]	17.4	15.7	18.0	18.8	36.0	19.0	15.4	18.0	18.6
10	0.09	0.23	0.93	0.13	2.24	0.54	0.90	0.25	1.05	0.20
13	26.5	32.4	35.8	33.4	34.4	39.5	31.4	33.6	35.7	31.6
14	0.03	2.45	0.20	0.30	4.06	5.10	1.49	0.34	0.04	0.08

[a] I, Leukaemia; II, non-small cell lung cancer; III, colon cancer; IV, CNS cancer; V, melanoma; VI, ovarian cancer; VII, renal cancer; VIII, prostate cancer; IX, breast cancer.

[b] GI$_{50}$ (μM) full panel mean-graph mid point (MG-MID) = the average sensitivity of all cell lines towards the test agent.

[c] Not tested.

values < 0.01 μM). Furthermore, compound **7a** showed also a remarkable sensitivity against most of the tested tumour cell lines with GI$_{50}$ values ranging between 1.94 and 27.5 μM. Except for the leukaemia subpanel, compounds **7b** and **9** exhibited almost the same pattern of sensitivity against most of the tested subpanel tumour cell lines with special pronounced activity against breast cancer MDA-MB-435 cell line (GI$_{50}$ values 4.93 and 16.8 μM, respectively). Although compound **13** proved to be less sensitive towards the nine subpanel tumour cell lines when compared with the pre-mentioned compounds, it showed an appreciable antitumor profile with GI$_{50}$ values ranging between 14.8 and 44.4 μM (Table 1).

With regard to the broad spectrum antitumor activity, the results revealed that all of the seven active compounds; **7a–c**, **9**, **11**, **13** and **14** showed effective growth inhibition GI$_{50}$ (MG-MID) values of 11.0, 20.9, 0.65, 18.6, 0.20, 31.6 and 0.08 μM, respectively, beside a cytostatic activity TGI (MG-MID) values of 44.7, 75.9, 41.6, 40.7, 11.7, 87.1 and 15.8 μM, respectively (Tables 2 and 3). In addition, except for compounds **7c** and **13**, the rest of the active compounds; **7a**, **7b**, **9**, **11**, **13** and **14**

exhibited cytotoxic activity with LC$_{50}$ (MG-MID) values of 85.1, 95.5, 79.4, 87.1 and 64.6 μM, respectively (Table 4).

Further interpretation of the obtained data revealed that, compounds **14** (GI$_{50}$, TGI, and LC$_{50}$ MG-MID values of 0.08, 15.8 and 64.6 μM, respectively) and **11** (GI$_{50}$, TGI, and LC$_{50}$ MG-MID values of 0.20, 11.7 and 87.1 μM, respectively) proved to be the most active members in this study with potential activity against all the tested subpanel tumour cell lines and particular effectiveness on the leukaemia subpanel at both the GI$_{50}$ (0.03 and 0.09 μM, respectively) and the TGI levels (35.2 and 28.1 μM, respectively) (Tables 2–4). Compound **7c** (GI$_{50}$ and TGI MG-MID values of 0.65 and 41.6 μM, respectively) displayed a remarkable growth inhibition and cytostatic effects when compared with **11** and **14**, however, it lacks cytotoxic activity (Tables 2 and 4). On the other hand, compounds **7a** (GI$_{50}$, TGI, and LC$_{50}$ MG-MID values of 11.0, 44.7 and 85.1 μM, respectively), **7b** (GI$_{50}$, TGI, and LC$_{50}$ MG-MID values of 20.9, 75.9 and 95.5 μM, respectively) and **9** (GI$_{50}$, TGI, and LC$_{50}$ MG-MID values of 18.6, 40.7 and 79.4 μM, respectively) displayed a considerable antitumor activity

Table 3
Median total growth inhibitory concentration (TGI, μM) and mean LC$_{50}$ (μM) values of in vitro subpanel tumour cell lines

Cpd. No.	Subpanel tumour cell lines [a]									MG-MID [b]
	I	II	III	IV	V	VI	VII	VIII	IX	
7a	99.0	50.4	30.7	56.3	54.2	43.9	57.3	– [c]	49.4	44.7
7b	–	70.0	84.0	74.5	66.2	87.3	90.8	–	81.7	75.9
7c	86.2	91.7	73.6	46.8	84.7	52.1	92.7	–	71.5	41.6
9	NT [d]	40.2	34.8	38.9	36.9	70.9	49.1	42.1	42.1	40.7
10	28.1	31.8	57.8	80.0	51.2	–	40.0	52.4	43.9	11.7
13	86.8	88.9	91.3	90.3	84.9	92.0	84.8	–	90.4	87.1
14	35.2	22.2	11.6	28.4	19.5	36.8	23.3	61.3	26.2	15.8

[a] For subpanel tumour cell lines see footnote (a) of Table 2.

[b] TGI (μM) full panel mean-graph mid point (MG-MID) = the average sensitivity of all cell lines towards the test agent.

[c] Subpanel TGI value > 100 μM.

[d] Not tested.

Table 4
Median lethal concentration 50 (LD$_{50}$, µM) values of in vitro subpanel tumour cell lines

Cpd. No.	Subpanel tumour cell lines [a]									MG-MID [b]
	I	II	III	IV	V	VI	VII	VIII	IX	
7a	– [c]	85.3	78.2	86.0	79.9	83.3	95.4	–	85.0	85.1
7b	–	96.6	92.7	96.1	94.5	95.0	–	–	–	95.5
7c	–	–	–	–	–	–	–	–	–	–
9	NT [d]	78.9	74.1	80.9	72.5	93.3	86.0	–	76.6	79.4
10	–	–	95.6	94.6	94.1	–	–	–	85.5	87.1
13	–	–	–	–	–	–	–	–	–	–
14	–	69.4	45.3	81.6	57.9	80.3	72.0	82.4	68.9	64.6

[a] For subpanel tumour cell lines see footnote (a) of Table 2.
[b] TGI (µM) full panel mean-graph mid point (MG-MID) = the average sensitivity of all cell lines towards the test agent.
[c] Subpanel LC$_{50}$ value > 100 µM.
[d] Not tested.

towards most of the tested tumour cell lines (Tables 2 and 4). Compound **13** was found to be the least effective antitumor agent in the present investigation with GI$_{50}$ and TGI MG-MID values of 31.6 and 87.1 µM, respectively; without any cytotoxic effect (Tables 2–4).

The ratio obtained by dividing the full panel MG-MID (µM) of the compounds by their individual subpanel MG-MID (µM) is considered as a measure of compound selectivity. Ratios between 3 and 6 refer to moderate selectivity, ratios greater than 6 indicate high selectivity towards the corresponding cell line, while compounds not meeting either of these criteria are rated non-selective [40]. All the active compounds in the present study proved to be non-selective with broad spectrum antitumor activity against the nine tumour subpanels tested with ratios ranging between 0.02 to 2.83 for the GI$_{50}$ and 0.15 to 1.36 for the TGI. At the GI$_{50}$ level, compounds **7c** and **14** revealed mild selectivity towards the leukaemia subpanel with selectivity ratios near 3 (2.8 and 2.7, respectively). Regarding the selectivity of the tested compounds against some of the individual subpanel tumour cell lines, compound **7a** was found to exhibit moderate selectivity towards leukaemia SR and breast MDA-MB-435 cancer cell lines at the GI$_{50}$ level with selectivity ratios of 3.7 and 5.7, respectively. This selectivity was retained at the TGI level for the latter cell line (selectivity ratio 8.9). Compound **7c** showed a significant high selectivity towards the same subpanel tumour cell lines at the GI$_{50}$ level with selectivity ratios of 65.0 and 20.0, respectively. Moreover, the same compound was proved to be highly selective towards CNS SF-295, ovarian OVCAR-3 and breast MCF7 cancer cell lines at the GI$_{50}$ (selectivity ratio 65.0 for the three cell lines) and TGI levels (selectivity ratios 102, 133 and 61, respectively). On the other hand, compounds **11** and **14** revealed high selectivity ratios ranging between 6.7 and 20.0 towards CNS SF-539, CNS U251, renal TK-10 and breast

MDA-MB-435 cancer cell lines at both the GI$_{50}$ and TGI levels.

Structurally, the tested compounds represent two different main hybrids, namely the 5-(1-(4-chlorophenyl)-4-hydroxy-1*H*-pyrazol-3-yl)-4-substituted-1,2,4-triazolin-3-thiones **7a–c** and the 5-(1-(4-chlorophenyl)-4-hydroxy-1*H*-pyrazol-3-yl)-2-substituted-1,3,4-oxadiazoles **9**, **11**, **13** and **14** (Figs. 2 and 3). Within the first series (Fig. 2), the substituent at position 4 of the 1,2,4-triazolin-3-thione moiety seems to modulate the antitumor activity. The cyclohexyl group (**7c**, R = cyclohexyl); was the most favourable substituent among this series. Thus, **7c** is considered to be the most active member within this series with distinctive antitumor activities against all the tested subpanel tumour cell lines (GI$_{50}$ and TGI MG-MID values of 0.65 and 41.6 µM, respectively), however without any cytotoxic effect. Replacement of the alicyclic group with an aromatic moiety as in **7a** (R = C$_6$H$_5$), resulted in a 2–5-fold reduction in the growth inhibitory activity against most of the tested subpanel tumour cell lines, except for the leukaemia subpanel which showed a dramatic reduction (82-fold) in activity. The antitumor activities against the ovarian, renal and breast cancer cell lines were marginally affected (Table 2). However, this compound revealed some cytotoxic activity with LC$_{50}$ value of 85.1 µM (Table 4). Substituting this phenyl group with a fluorine atom as in **7b** (R = 4-F-C$_6$H$_4$), decreased the full panel activity by 2-fold at both the GI$_{50}$ and TGI levels (Tables 2 and 3) and showed 2–3-fold reduction in activity against most of the tested subpanel tumour cell lines except for the leukaemia, melanoma and prostate cancer subpanels where the activity was retained nearly within the same level (Table 2). The higher growth inhibitory and cytostatic activities of **7c** relative to **7a** and **7b** are concordant with some previous reports [41–43] which have discussed the biological significance of the cyclohexyl moiety rather than other aromatic substituents in enhancing the antitumor properties of

such type of 1,2,4-triazolin-3-thiones attached to a variety of heterocyclic ring systems.

Regarding the 2-substituted-1,3,4-oxadiazoles structure variants **9**, **11**, **13** and **14**; the antitumor activity of these compounds appears to be closely related to the nature of the substituent at position-2 of the 1,3,4-oxadiazole counterpart. Compound **14**; 5-(1-(4-chlorophenyl)-4-hydroxy-1*H*-pyrazol-3-yl)-2-phenyl-1,3,4-oxadiazole (Fig. 3); was proved to be the most active member with a unique antitumor potency against all the tested subpanel tumour cell lines (GI_{50}, TGI, and LC_{50} MG-MID values of 0.08, 15.8 and 64.6 μM, respectively) (Tables 2–4). Separation of the phenyl group at position 2 from the 1,3,4-oxadiazole counterpart with an NH linker as in **9** (Fig. 2), resulted in an obvious reduction in activity (GI_{50}, TGI, and LC_{50} MG-MID values of 18.6, 40.7 and 79.4 μM, respectively), against all the tested subpanel tumour cell lines except for leukaemia, at both the GI_{50} and TGI levels (Tables 2 and 3). Here, it should be pointed out that replacing the 1,3,4-oxadiazole with its isosteric 1,3,4-thiadiazole ring system as in **8** (Fig. 2), led to a total loss of the antitumor activity. Furthermore, replacing the aromatic moiety in **14** with an oxo function as in **11**; 5-(1-(4-chlorophenyl)-4-hydroxy-1*H*-pyrazol-3-yl)-1,3,4-oxadiazol-2-one (Fig. 3); led to a highly active analogue with GI_{50}, TGI, and LC_{50} MG-MID values of 0.2, 11.7 and 87.1 μM, respectively (Tables 2 and 4). When compared with **14**, this analog showed 2–10-fold improvement in the antitumor activity against most of the tested subpanel tumour cell lines, except for the leukaemia and the breast cancer subpanels which showed 3- and 25-fold reduction in activity, respectively. It is worth mentioning that, isosteric replacement of the 2-oxo with 2-thioxo function as in **10** (Fig. 3), led to complete abolishment of the antitumor activity. On the other hand, the 3-acetyl-5-(4-acetyloxy-1-(4-chlorophenyl)-1*H*-pyrazol-3-yl)-2-(2,4-difluorophenyl)-1,3,4-oxadiazoline **13** (Fig. 3); proved to be the least active member among the substituted 1*H*-pyrazolyl-1,3,4-oxadiazole analogs with GI_{50} and TGI MG-MID values of 31.6 and 87.1 μM, respectively and without any cytotoxic activity (Tables 2–4). Such reduction in the biological activity might be attributed to the acetylation of the 4-hydroxyl group of the 1*H*-pyrazole as well as the 1,3,4-oxadiazoline ring which would block an active hydrogen-bond forming centre in the molecule. This suggestion was intensified by the fact that the diacetyl pyrazole derivative **3** (Fig. 2) proved to be totally inactive in vitro under the same experimental conditions. Collectively, these results highlight the synergestic role of the 4-hydroxy-1*H*-pyrazole nucleus together with the substitution pattern of the 1,3,4-oxadiazole counterpart in manipulating the enhanced biological activity of such model of compounds.

3.2. In vitro effect on the replication of hepatitis-C virus in HCV-infected HepG2 heptocellular carcinoma cell line

Compounds **2–5**, **6a–d**, **7a**, **8–11**, **12a**, **13**, and **14** were investigated for their in vitro effect on the replication of HCV in HepG2 heptocellular carcinoma cell line infected with the virus. In the last few years, a number of cell culture systems have been developed that support reliable and efficient progression of this virus. Among several human hepatocyte cell lines analysed, the hepatocellular carcinoma HepG2 cell line was found to be most susceptible to the HCV infection [44]. On the other hand, monitoring of the HCV viremia pre- and post-antiviral therapy through the detection of viral (+) and/or (−) RNA strands by the use of qualitative reverse transcription-polymerase chain reaction (RT-PCR) has become the most frequently-used, reliable and sensitive technique. Recently, it has been reported that the detection of the (−) strand HCV RNA using the RT-PCR is a very important tool for understanding the life cycle of the HCV and provides a reliable marker for the diagnosis of HCV and monitoring the viral response to antiviral therapy [45].

Based on these facts, the adopted protocol in the present study contributes to the simultaneous detection of the (+) and/or (−) HCV RNA strands in HepG2 hepatoma cells infected with HCV. Inhibition of viral replication was detected by amplification of viral RNA segments using the RT-PCR technique, both in the uninfected cultivated cells (as a positive control) and in the presence of variable concentrations (10, 25, 50 and 100 μg mL^{-1}) of the test compound at optimal temperature. The test compound is considered to be active when it is capable of inhibiting the viral replication inside the HCV-infected HepG2 cells, as evidenced by the disappearance of the (+) and/or (−) strands viral RNA-amplified products detected by the RT-PCR (compared with the positive control).

Out of the compounds tested, only two derivatives namely; the *N*-formyl-1-(4-chlorophenyl)-4-hydroxy-1*H*-pyrazole-3-carboxylic acid hydrazide **2** and 1-(1-(4-chlorophenyl)-4-hydroxy-1*H*-pyrazole-3-carbonyl)-thiosemicarbazide **5** proved to inhibit the viral replication inside HCV-infected hepatoma HepG2 cell line as revealed from their corresponding gel pictures illustrated in Figs. 4 and 5. The *N*-formyl derivative **2** was able to inhibit the replication of the (+) strand HCV RNA at a dose of 100 μg mL^{-1} as indicated by the absence of the amplified PCR products at lane 5 (Fig. 4). On the other hand, the thiosemicarbazide **5** exhibited a distinctive HCV inhibitory profile as revealed from Fig. 5, where no (+) or (−) viral RNA products were detected at lower doses (25 and 50 μg mL^{-1}). At the 10 μg mL^{-1} dose level, the compound inhibited the replication of the (+) strand HCV RNA rather than the (−) strand. It is worth mentioning that
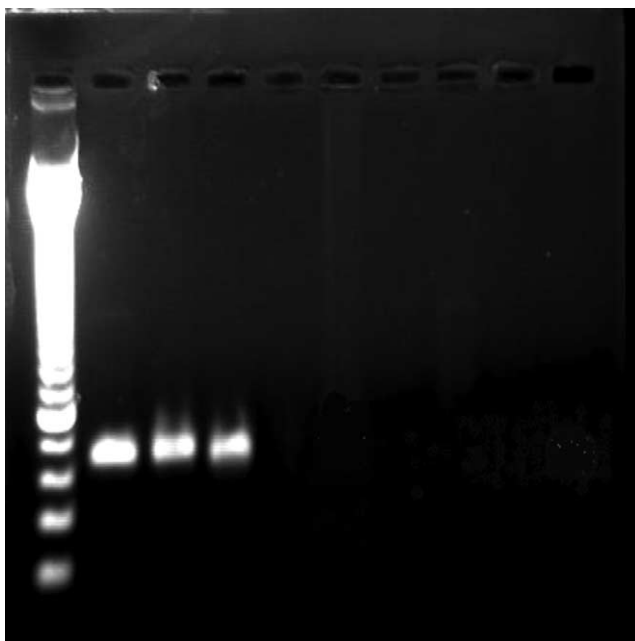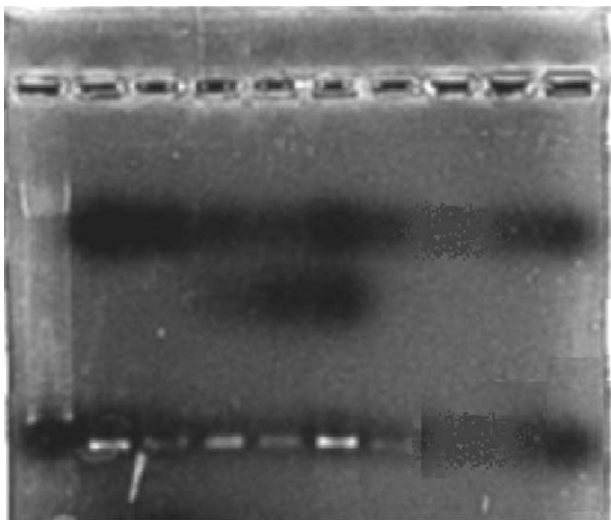
Fig. 4. PCR amplification picture of HCV RNA (+) and (−) strands in the presence of compound 2. Lane 1 is the molecular weight marker (MWM) 50bp ladder. Lane 2 = control (C). Lanes 3, 5, 7, 9 are the effect of compound 2 (10, 25, 50, 100 μg, respectively) on the HCV RNA (+) strand. Lanes 4, 6, 8, 10 are the effect of compound 2 (10, 25, 50, 100 μg, respectively) on the HCV RNA (−) strand.

Fig. 5. PCR amplification picture of HCV RNA (+) and (−) strands in the presence of compound 5. Lane 1 is the molecular weight marker (MWM) 50bp ladder. Lane 2 = control (C). Lanes 3, 5, 7, 9 are the effect of compound 5 (10, 25, 50, 100 μg, respectively) on the HCV RNA (+) strand. Lanes 4, 6, 8, 10 are the effect of compound 5 (10, 25, 50, 100 μg, respectively) on the HCV RNA (−) strand.

the substituted thiosemicarbazides **6a**–**d** and the *N*-phenylsemicarbazide **4** failed to exhibit any antiviral activity under the same test conditions and dose level used.

4. Conclusion

In conclusion, the aim of the present research work was to synthesize novel 1*H*-pyrazole lead compounds possessing potential antitumor as well as anti-HCV activities and are structurally related to the natural 4-hydroxypyrazole; pyrazofurin. Our aim has been achieved by the synthesis of two different groups of structure hybrids comprising the 4-hydroxy-1*H*-pryazole moiety with either the 4-substituted-1,2,4-triazolin-3-thione (compounds **7a**–**c**) or the 2-substituted-1,3,4-oxadiazole (compounds **9**, **11**, **13** and **14**) counterparts in one and the same entity for synergistic purpose. The most active seven compounds at the GI_{50} level exhibited TGI levels with nearly the same order of activity; **14** > **11** > **7c** > **7a** > **7b** ≈ **9** > **13** (Tables 2 and 3). Compounds **11** and **14** proved to be the most active derivatives identified in this study as evidenced by their potential growth inhibitory, cytostatic and cytotoxic activities, regardless to the subpanel being tested, with special high selectivity profile against some individual cell lines. Compounds **11** and **7c** were selected by the NCI Developmental Therapeutic Program for further in vitro biological evaluation. Interestingly, compound **14** is currently under review by the NCI Biological Evaluation Committee at the last stage of the in vitro screening. On the other hand, compounds **2** and **5** revealed potential inhibitory effect on the replication of the HCV RNA (+) and (−) strands in HepG2 hepatocellular carcinoma cell line infected with the HCV at 10–100 μg mL^{-1} concentration range in the RT-PCR experimental protocol. All these favourable features make such type of 4-hydroxypyrazole derivatives the appropriate candidates for future testing and derivatisation in the hope of finding more selective and active anticancer and antiviral compounds in the nanomolar concentration level or less.
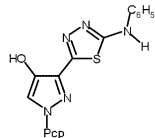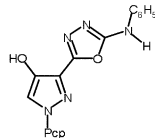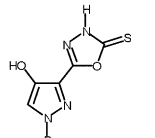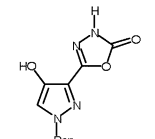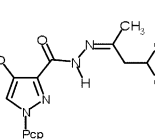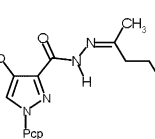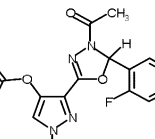
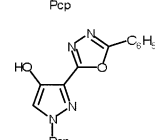## 5. Experimental
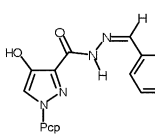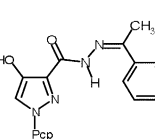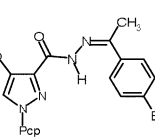
5.1. Chemistry

Melting points were determined in open-glass capillaries on a Stuart melting point apparatus and were uncorrected. The infrared (IR) spectra were recorded on 470-Shimadzu infrared spectrophotometer using the KBr disc technique. The ^{1}H-NMR (δ-ppm) spectra were recorded on a Bruker (500 MHz) spectrometer using tetramethylsilane as the internal standard and

Table 5
Physical and analytical data of compounds **2–14**

Cpd. No.	Structural Formula	M.P. (°C)*	Yield (%)	Mol. Formula	Mol. Weight**
2		223-25[a]	80.4	$C_{11}H_9ClN_4O_3$	280.67
3		166-68[a]	87.5	$C_{14}H_{13}ClN_4O_4$	336.73
4		222-24[a]	44.4	$C_{17}H_{14}ClN_5O_3$	371.78
5		252-54[a]	30	$C_{11}H_{10}ClN_5O_2S$	311.75
6a		210-12[a]	84	$C_{17}H_{14}ClN_5O_2S$	387.84
6b		235-37[a]	61.7	$C_{17}H_{13}ClFN_5O_2S$	405.83
6c		200-02[a]	57	$C_{17}H_{20}ClN_5O_2S$	393.89
6d		203-05[a]	81	$C_{14}H_{14}ClN_5O_2S$	351.81
7a		285-87[a]	90	$C_{17}H_{12}ClN_5OS$	369.83
7b		266-68[a]	85	$C_{17}H_{11}ClFN_5OS$	387.82
7c		280-82[a]	88	$C_{17}H_{18}ClN_5OS$	375.88

8		239-41[b]	90	$C_{17}H_{12}ClN_5OS$	369.83
9		228-30[a]	31	$C_{17}H_{12}ClN_5O_2$	353.76
10		148-50[a]	83.3	$C_{11}H_7ClN_4O_2S$	294.72
11		>300[b]	60	$C_{11}H_7ClN_4O_3$	278.65
12a		260-62[c]	66.3	$C_{17}H_{11}ClF_2N_4O_2$	376.74
12b		257-59[c]	51.2	$C_{18}H_{15}ClN_4O_2$	354.79
12c		273-75[d]	53.9	$C_{18}H_{14}BrClN_4O_2$	433.69
12d		270-72[c]	30	$C_{16}H_{19}ClN_4O_2$	334.8
12e		280-82[c]	56.5	$C_{20}H_{19}ClN_4O_2$	382.84
13		165-67[a]	70	$C_{21}H_{15}ClF_2N_4O_4$	460.82
14		163-65[e]	75	$C_{17}H_{11}ClN_4O_2$	338.75

* Crystalization solvents: a, ethanol; b, DMF/water; c, ethanol/water; d, acetic acid; e, DMF/ethanol
** Analyzed for C, H, N, S; results are within 0.4% of the theoretical values for the formulae givin.
Pcp = P-clorophenyl.

DMSO-d_6 as the solvent. Splitting patterns were designated as follows: s; singlet; d: doublet; m: multiplet. Mass spectra were recorded on a Finnigan SSQ 7000 GC–MS, ionisation energy 70 eV. Elemental analyses were performed at the Microanalytical Unit, Faculty of Science, Cairo University, Cairo, Egypt, and the found values were within ±0.4% of the theoretical values. Follow up of the reactions and checking the homogeneity of the compounds were made by TLC on silica gel-protected aluminium sheets (Type 60 F254, Merck) and the spots were detected by exposure to UV-lamp at λ 254 nm for a few seconds. Compound **1** was synthesized as described in Ref. [18].

5.1.1. N-Formyl-1-(4-chlorophenyl)-4-hydroxy-1H-pyrazole-3-carboxylic acid hydrazide (2)

A solution of 1-(4-chlorophenyl)-4-hydroxy-1H-pyrazole-3-carboxylic acid hydrazide **1** (0.5 g, 2 mmol) in formic acid (5 mL) was heated under reflux for 1 h, during which a yellow solid was partially crystallized out. After being cooled to room temperature, the product was filtered, washed and recrystallised. Physical and analytical data are recorded in Table 5. IR (cm^{-1}): 3145–2930 (OH, NH), 1667 (C=O aldehyde), 1630 (C=O amide), 1593, 1496, 1377 (C=C, C=N, amide II, aromatics), 829 (C–Cl). ^{1}H-NMR: δ 10.12 (s, 1H, N*H*), 8.1 (s, 1H, pyrazole–C$_5$–*H*), 8.0 (s, 1H, C*H*O), 7.91 (d, 2H, Ar–*H*), 7.55 (d, 2H, Ar–*H*). MS, *m/z* (%): 282.0 (5.5), 280.0 (16.9, M$^+$), 254.0 (5.6), 252.0 (16.9), 223.0 (33.1), 221.0 (100), 140.0 (16.4), 137.9 (49.6), 112.9 (16.8), 111.0 (53.4), 77.0 (5.0), 75.0 (25.2).

5.1.2. N-Acetyl-4-acetyloxy-1-(4-chlorophenyl)-1H-pyrazole-3-carboxylic acid hydrazide (3)

The acid hydrazide **1** (0.5 g, 2 mmol) was warmed with acetic anhydride (5 mL) for 1 h, then the mixture was allowed to attain room temperature. The deposited yellow solid was filtered, washed with pet. ether (60–80 °C) and recrystallised. Physical and analytical data are listed in Table 5. IR (cm^{-1}): 3550–3105 (NH), 1758 (C=O acetyl), 1734 (C=O acetyl), 1667 (C=O amide), 1655, 1544, 1497, 1475, 1427 (C=C, C=N, amide II, aromatics), 1252 (C–O–C), 831 (C–Cl). ^{1}H-NMR: δ 8.8 (s, 1H, pyrazole–C$_5$–*H*), 7.81 (d, 2H, Ar–*H*), 7.63 (d, 2H, Ar–*H*), 2.56 (s, 3H, C*H$_3$*), 2.34 (s, 3H, C*H$_3$*). MS, *m/z* (%): 339.1 (6.6), 338.0 (15.9), 337.1 (20.8), 336.0 (41.1, M$^+$), 296.0 (29.9), 294.0 (79.4), 281.0 (20.3), 279.0 (62.4), 265.0 (29.8), 263 (80.4), 254.0 (34.4), 252.0 (89.8), 223.0 (59.4), 220.9 (100), 139.9 (19.1), 137.9 (54.9), 127.0 (37.1), 125.0 (83.9), 112.0 (14.3), 110.0 (44.6), 101.0 (7.6), 99.0 (22.6), 77.0 (2.0), 75.0 (16.7).

5.1.3. 4-Phenyl-1-(1-(4-chlorophenyl)-4-hydroxy-1H-pyrazole-3-carbonyl)semicarbazide (4)

To a solution of the acid hydrazide **1** (0.5 g, 2 mmol) in ethanol (10 mL), was added phenyl isocyanate (0.3 g,

2.5 mmol). The reaction mixture was refluxed for 1 h, then allowed to attain room temperature. The separated solid was filtered, washed with cold ethanol and recrystallised. Physical and analytical data are listed in Table 5. IR (cm^{-1}): 3670–2860 (OH, NH), 1729 (C=O), 1617 (C=O), 1578, 1553, 1496 (C=C, C=N, amide II, aromatics), 827 (C–Cl). ^{1}H-NMR: δ 9.3–9.2 (m, 3H, N*H*), 8.2 (s, 1H, pyrazole-C$_5$-*H*), 8.0–7.26 (m, 9H, Ar-*H*).

5.1.4. 1-(1-(4-Chlorophenyl)-4-hydroxy-1H-pyrazole-3-carbonyl)-thiosemicarbazide (5)

A mixture of **1** (0.5 g, 2 mmol) and ammonium thiocyanate (0.45 g, 6 mmol) in hydrochloric acid (20%, 20 mL) was heated under reflux for 3h. The reaction mixture was concentrated, cooled and the separated solid was filtered, washed with water, dried and recrystallised. Physical and analytical data are listed in Table 5. IR (cm^{-1}): 3375–2655 (OH, NH), 1667 (C=O), 1593, 1571, 1531, 1499, 1460 (C=C, C=N, amide II, aromatics), 994 (NCS), 824 (C–Cl). ^{1}H-NMR: δ 9.95 (s, 1H, CON*H*), 9.3 (s, 1H, CSN*H*), 8.1 (s, 1H, pyrazole–C$_5$–*H*), 7.75–7.3 (m, 6H, Ar–*H* and CSN*H$_2$*).

5.1.5. 4-Substituted-1-(1-(4-chlorophenyl)-4-hydroxy-1H-pyrazole-3-carbonyl)thiosemicarbazides (6a–d)

To a solution of the acid hydrazide **1** (1 g, 4 mmol) in ethanol (20 mL) was added the appropriate isothiocyanate (5 mmol). The reaction mixture was refluxed for 6–8 h, then allowed to attain room temperature. The separated solid was filtered, washed with cold ethanol and recrystallised. Physical and analytical data are listed in Table 5. IR (cm^{-1}): 3470–2935 (OH, NH), 1665 (C=O), 1593, 1555, 1531, 1494, 1460 (C=C, C=N, amide II, aromatics), 982–958 (NCS), 850–829 (C–Cl). ^{1}H-NMR of **6c**: δ 9.69–9.3 (m, 2H, N*H*), 8.1 (s, 1H, pyrazole–C$_5$–*H*), 7.96 (d, 2H, Ar–*H*), 7.9 (s, 1H, N*H*), 7.65 (d, 2H, Ar–*H*), 4.1 (s, 1H, cyclohexyl–*H*), 1.79–1.03 (m, 10H, cyclohexyl–*H*).

5.1.6. 5-(1-(4-Chlorophenyl)-4-hydroxy-1H-pyrazol-3-yl)-4-substituted-1,2,4-triazolin-3-thiones (7a–c)

The appropriate 4-substituted-1-(1-(4-chlorophenyl)-4-hydroxy-1H-pyrazole-3-carbonyl)-thiosemicarbazide **6a–c** (1 mmol) in sodium hydroxide (2N, 10 mL) was heated under reflux for 4 h, cooled, neutralized to pH 6 using dilute hydrochloric acid. The separated solid product was filtered, washed with water, dried and recrystallised. Physical and analytical data are listed in Table 5. IR (cm^{-1}): 3530–2800 (OH, NH), 1618, 1591, 1567, 1496 (C=C, C=N, aromatics), 1375–1317 (NCS), 834–824 (C–Cl). ^{1}H-NMR of **7a**: δ 14.12 (s, 1H, O*H*), 9.31 (s, 1H, N*H*), 8.0 (s, 1H, pyrazole-C$_5$-*H*), 7.92–7.33 (m, 10H, N*H* and Ar-*H*). MS, *m/z* (%) of **7c**: 377.2 (14.7), 375.2 (38.3, M$^+$), 296.0 (11.2), 295.0 (38.8), 294.1 (30.7), 293.0 (100), 222.0 (2.3), 220.0 (6.3), 169.0 (5.9),

167.0 (18.0), 141.0 (12.5), 140.0 (29.1), 139.0 (37.7), 138.0 (73.4), 132.0 (26.8), 129.0 (20.2), 128.0 (67.5), 127.0 (76.2), 112.9 (17.1), 111.0 (52.3), 83.1 (3.5), 81.1 (12.2), 77.0 (10.3), 75.0 (22.6).

5.1.7. 5-(1-(4-Chlorophenyl)-4-hydroxy-1H-pyrazol-3-yl)-2-phenylamino-1,3,4-thiadiazole (**8**)

To an ice-cold stirred solution of 1-(1-(4-chlorophenyl)-4-hydroxy-1*H*-pyrazole-3-carbonyl)-4-phenylthiosemicarbazide **6a** (0.5 g, 1.3 mmol) in absolute ethanol (10 mL), sulphuric acid (5 mL) was carefully added over a period of 15 min. Stirring was maintained at room temperature for 4 h then the reaction mixture was poured carefully to an equal volume of ice water. The precipitate formed was filtered, washed with water, dried and recrystallised. Physical and analytical data are listed in Table 5. IR (cm^{-1}): 3380–3145 (OH, NH), 1653, 1599, 1552, 1496 (C=C, C=N, aromatics), 831 (C–Cl). ^{1}H-NMR: δ 10.13 (s, 1H, O*H*), 9.77 (s, 1H, N*H*), 8.12 (s, 1H, pyrazole–C$_5$–*H*), 7.93 (d, 2H, Ar–*H*), 7.58 (d, 2H, Ar–*H*), 7.49–7.14 (m, 5H, Ar–*H*). MS, *m/z* (%): 369.1 (2.0, M$^+$), 296.0 (2.1), 294.0 (5.7), 254.0 (19.1), 252.0 (56.5), 224.0 (4.5), 223.0 (40.5), 222.0 (14.2), 221.0 (100), 140.0 (12.5), 139.0 (37.7), 137.9 (73.8), 135.0 (79.6), 112.9 (12.5), 111.0 (38.9), 93.0 (14.6), 77.0 (47.0), 75.0 (20.5).

5.1.8. 5-(1-(4-Chlorophenyl)-4-hydroxy-1H-pyrazol-3-yl)-2-phenylamino-1,3,4-oxadiazole (**9**)

Finely-powdered yellow mercuric oxide (0.4 g, 1.8 mmol) was, portionwise, added over a period of 30 min to a boiling solution of 1-(1-(4-chlorophenyl)-4-hydroxy-1*H*-pyrazole-3-carbonyl)-4-phenylthiosemicarbazide **6a** (0.5 g, 1.3 mmol) in absolute ethanol (20 mL). The resulting suspension was heated under reflux for 2 h, then filtered while hot. The black precipitate was washed three times with boiling ethanol (3 × 10 mL) and the combined filtrate and washings were concentrated to a small volume and set aside for an overnight at room temperature. The separated product was filtered, dried and recrystallised. Physical and analytical data are listed in Table 5. IR (cm^{-1}): 3320–3120 (OH, NH), 1630, 1593, 1552 (C=C, C=N, aromatics), 830 (C–Cl). ^{1}H-NMR: δ 10.0 (s, 1H, O*H*), 9.47 (s, 1H, N*H*), 8.1 (s, 1H, pyrazole–C$_5$–*H*), 7.83–7.11 (m, 9H, Ar–*H*). MS, *m/z* (%): 355.1 (34.1), 353.1 (100, M$^+$), 254.0 (8.1), 252.0 (25.9), 224.0 (2.6), 223.0 (21.9), 222.0 (9.2), 221.0 (73.1), 220.0 (3.4), 219.0 (14.9), 188.0 (14.8), 187.0 (46.0), 169.0 (5.6), 166.9 (17.1), 141.0 (13.9), 140.0 (34.1), 138.9 (42.6), 138.0 (97.9), 134.9 (47.9), 132.0 (31.3), 118.0 (20.4), 117.0 (15.9), 112.9 (27.6), 112.0 (11.4), 110.9 (85.4), 93.0 (19.4), 92.0 (22.7), 91.0 (10.5), 77.0 (82.3), 75.0 (41.5).

5.1.9. 5-(1-(4-Chlorophenyl)-4-hydroxy-1H-pyrazol-3-yl)-1,3,4-oxadiazolin-2-thione (**10**)

The acid hydrazide **1** (0.5 g, 2 mmol) was dissolved in a solution of potassium hydroxide (0.11 g, 2 mmol) in water (2 mL) and ethanol (20 mL). Carbon disulfide (2 mL) was then added while stirring and the reaction mixture was heated under reflux for 8 h. The solvents were removed under reduced pressure, the residue was treated with water then filtered. The filtrate was cooled, neutralized to pH 6 using dilute hydrochloric acid and the separated product was filtered, washed with water, dried and recrystallised. Physical and analytical data are listed in Table 5. IR (cm^{-1}): 3555–3000 (OH, NH), 1628, 1545, 1495 (C=C, C=N, aromatics), 1374 (C=S), 823 (C–Cl). ^{1}H-NMR: δ 10.4 (s, 1H, O*H*), 9.66 (s, 1H, N*H*), 8.2 (s, 1H, pyrazole–C$_5$–*H*), 7.76–7.23 (m, 4H, Ar–*H*). MS, *m/z* (%): 296.2 (9.2), 294.1 (25.2, M$^+$), 239.1 (4.3), 238.1 (23.8), 237.1 (9.8), 236.1 (81.2), 224.2 (2.5), 223.1 (14.5), 222.1 (5.4), 221.1 (42.6), 149.0 (13.7), 141.1 (4.5), 140.0 (16.8), 139.1 (10.3), 138.1 (47.5), 129.1 (19.7), 128.1 (19.0), 127.1 (58.2), 126.1 (40.6), 125.1 (100), 114.1 (4.1), 113.0 (25.8), 112.0 (11.4), 111.0 (77.8), 105.1 (28.9), 101.0 (20.8), 99.0 (59.5), 97.1 (30.1), 93.0 (6.8), 92.0 (22.7), 91.0 (18.3), 77.0 (33.8), 75.0 (57.6).

5.1.10. 5-(1-(4-Chlorophenyl)-4-hydroxy-1H-pyrazol-3-yl)-1,3,4-oxadiazolin-2-one (**11**)

To an ice-cold stirred solution of the acid hydrazide **1** (0.5 g, 2 mmol) and triethylamine (0.5 mL) in tetrahydrofuran (30 mL) was added 1,1′-carbonyldiimidazole (CDI) (0.48 g, 3 mmol). Stirring at 0 °C was continued for 5 h then the reaction mixture was treated with additional amounts of triethylamine (0.5 mL) and CDI (0.48 g, 3 mmol), then stirring was maintained at room temperature for an overnight. The solvent was evaporated to dryness under reduced pressure, the residue was treated with ethanol then filtered. The resulting precipitate was washed with ethanol, dried and recrystallised. Physical and analytical data are listed in Table 5. IR (cm^{-1}): 3650–2995 (OH, NH), 1778 (C=O), 1665, 1631, 1590, 1495 (C=C, C=N, aromatics), 1250 (C–O–C), 823 (C–Cl). ^{1}H-NMR: δ 10.3 (s, 1H, O*H*), 9.7 (s, 1H, N*H*), 8.1 (s, 1H, pyrazole–C$_5$–*H*), 7.82–7.33 (m, 4H, Ar–*H*). MS, *m/z* (%): 280.1 (5.5), 278.0 (17.1, M$^+$), 254.1 (3.8), 252.1 (12.2), 239.1 (2.1), 238.2 (5.9), 237.1 (6.8), 236.0 (14.4), 224.1 (3.2), 223.1 (25.1), 222.0 (12.6), 221.0 (84.3), 141.0 (11.5), 140.0 (40.0), 139.0 (27.2), 138.0 (97.9), 129.0 (6.6), 128.0 (6.5), 127.0 (18.0), 126.0 (18.3), 125.0 (34.6), 114.0 (5.5), 112.9 (40.7), 112.0 (18.5), 111.0 (100), 101.0 (9.0), 99.0 (16.6), 77.0 (14.3), 75.0 (55.0).

5.1.11. 3-(Alkylidenehydrazinocarbonyl)-1-(4-chlorophenyl)-4-hydroxy-1H-pyrazoles (**12a−e**)

A solution of **1** (0.5 g, 2 mmol) and the appropriate aldehyde or ketone (2 mmol) in gl. acetic acid (10 mL)

was refluxed for 6–8 h. The solid separated upon cooling was filtered, washed with cold ethanol and recrystallised. Physical and analytical data are listed in Table 5. IR (cm^{-1}): 3540–2775 (OH, NH), 1689–1649 (C=O), 1638, 1612, 1591, 1561, 1532, 1494, (C=C, C=N, amide II, aromatics), 840–821 (C–Cl). ^{1}H-NMR of **12e**: δ 9.99 (s, 1H, O*H*), 9.7 (s, 1H, N*H*), 8.11 (s, 1H, pyrazole-C$_5$-*H*), 7.9–755 (m, 9H, Ar-*H*), 3.29 (m, 4H, C*H$_2$*–C*H$_2$*), 1.9 (s, 3H, C*H$_3$*). MS, *m/z* (%) of **12a**: 378.1 (12.1), 376.1 (30.0, M$^+$), 239.0 (6.7), 237.0 (19.4), 224.0 (4.7), 223.0 (41.6), 222.0 (26.3), 221.0 (100), 141.0 (9.0), 140.0 (45.0), 139.0 (23.5), 138.0 (85.5), 128.0 (2.8), 127.0 (2.7), 126.0 (12.1), 125.0 (13.1), 114.0 (4.3), 112.9 (31.3), 111.9 (9.2), 110.9 (68.3), 101.0 (6.8), 100.0 (17.1), 77.0 (6.9), 75.0 (28.2).

5.1.12. 3-Acetyl-5-(4-acetyloxy-1-(4-chlorophenyl)-1H-pyrazol-3-yl)-2-(2,4-difluorophenyl)-1,3,4-oxadiazoline (13)

A mixture of 3-(2,4-difluorophenylidenehydrazino-carbonyl)-1-(4-chlorophenyl)-4-hydroxy-1*H*-pyrazole **12a** (0.4 g, 1 mmol) and acetic anhydride (5 mL) was heated under reflux for 1 h. After the reaction mixture was attained room temperature, excess acetic anhydride was decomposed by water and the mixture was stirred for further 30 min. The separated product was filtered, washed with water, dried and recrystallised. Physical and analytical data are listed in Table 5. IR (cm^{-1}): 1765 (C=O), 1660 (C=O), 1616, 1499, 1439 (C=C, C=N, aromatics), 1210 (C–O–C), 821 (C–Cl). ^{1}H-NMR: δ 8.8 (s, 1H, pyrazole–C$_5$–*H*), 7.87–7.33 (m, 7H, Ar–*H*), 7.1 (s, 1H, oxadiazole–C$_2$–H), 2.3 (s, 3H, C*H$_3$*), 2.21 (s, 3H, C*H$_3$*). MS, *m/z* (%): 462.1 (4.0), 460.1 (12.2, M$^+$), 378.1 (7.3), 376.1 (21.2), 265.0 (11.0), 263.0 (33.6), 239.0 (6.9), 237.0 (21.2), 224.0 (3.6), 223.0 (33.0), 222.0 (18.7), 221.0 (100), 141.0 (6.2), 140.0 (21.4), 139.0 (9.8), 138.0 (46.0), 112.9 (12.6), 111.0 (32.1), 100.0 (10.6), 75.0 (10.9).

5.1.13. 5-(1-(4-Chlorophenyl)-4-hydroxy-1H-pyrazol-3-yl)-2-phenyl-1,3,4-oxadiazole (14)

To a cooled mixture of equimolar amounts of the acid hydrazide **1** (0.5 g, 2 mmol) and benzoic acid (0.24 g, 2 mmol) was added phosphorous oxychloride (5 mL) while stirring. The reaction mixture was then heated under reflux for 2 h, cooled, poured carefully to an equal volume of ice water then neutralized with solid sodium bicarbonate. The precipitate formed after standing for 1 h was filtered, washed with water, dried and recrystallised. Physical and analytical data are listed in Table 5. IR (cm^{-1}): 3450–3015 (OH), 1657, 1560, 1495, 1458 (C=C, C=N, aromatics), 1111 (C–O–C), 825 (C–Cl). ^{1}H-NMR: δ 9.8 (s, 1H, O*H*), 8.2 (s, 1H, pyrazole–C$_5$–*H*), 7.79–7.18 (m, 9H, Ar–*H*). MS, *m/z* (%): 340.2 (33.9), 338.2 (100, M$^+$), 254.1 (12.9), 252.0 (26.6), 224.1 (2.7), 223.1 (21.6), 222.1 (10.6), 221.1 (64.1), 173.1

(15.0), 172.1 (58.2), 169.1 (6.7), 167.1 (15.2), 141.1 (13.7), 140.1 (28.6), 139.1 (39.7), 138.1 (79.0), 132.1 (26.8), 114.0 (3.6), 113.0 (22.6), 112.0 (9.4), 111.0 (69.0), 105.1 (48.1), 103.1 (17.6), 78.1 (5.1), 77.1 (68.6), 76.1 (15.6), 75.1 (34.7).

5.2. In vitro antitumor screening

Compounds **3**, **7a–c**, **8–11**, **13** and **14** were subjected to the NCI in vitro disease-oriented human cells screening panel assay to screen their antitumor activities. About 60 cell lines of nine tumour subpanels, including leukaemia, non-small cell lung, colon, CNS, melanoma, ovarian, renal, prostate and breast cancer cell lines were utilized. The human tumour cell lines of the cancer screening panel were grown in RPMI 1640 medium containing 5% foetal bovine serum and 2 mM L-glutamine. For a typical screening experiment, cells were inoculated into 96-well microtiter plates in 100 mL at plating densities ranging from 5000 to 40 000 cells/well depending on the doubling time of individual cell lines. After cell inoculation, the microtiter plates were incubated at 37 °C, 5% CO$_2$, 95% air and 100% relative humidity for 24 h prior to addition of experimental drugs. After 24 h, two plates of each cell line were fixed in situ with TCA, to represent a measurement of the cell population for each cell line at the time of drug addition. Experimental drugs were solubilised in dimethyl sulphoxide at 400-fold the desired final maximum test concentration and stored frozen prior to use. At the time of drug addition, an aliquot of frozen concentrate was thawed and diluted to twice the desired final maximum test concentration with complete medium containing 50 mg mL^{-1} gentamicin. Additional four, 10-fold or 1/2 log serial dilutions were made to provide a total of five drug concentrations plus control. Aliquots of 100 mL of these different drug dilutions were added to the appropriate microtiter wells already containing 100 mL of medium, resulting in the required final drug concentrations. Following drug addition, the plates were incubated for an additional 48 h at 37 °C, 5% CO$_2$, 95% air, and 100% relative humidity. For adherent cells, the assay was terminated by the addition of cold TCA. Cells were fixed in situ by the gentle addition of 50 mL of cold 50% (w/v) TCA (final concentration, 10% TCA) and incubated for 60 min at 4 °C. The supernatant was discarded, and the plates were washed five times with tap water and air dried. Sulphorhodamine B (SRB) solution (100 mL) at 0.4% (w/v) in 1% acetic acid was added to each well, and plates were incubated for 10 min room temperature. After staining, unbound dye was removed by washing five times with 1% acetic acid and the plates were air dried. Bound stain was subsequently solubilised with 10 mM trizma base, and the absorbance was read on an automated plate reader at a wavelength of 515 nm. For

suspension cells, the methodology was the same except that the assay was terminated by fixing settled cells at the bottom of the wells by gently adding 50 mL of 80% TCA (final concentration, 16% TCA). Three response parameters (GI_{50}, TGI, and LC_{50}) were calculated for each cell line [37–39].

5.3. In vitro effect on the replication of hepatitis-C virus in HCV-infected HepG2 heptocellular carcinoma cell line

5.3.1. Cell culture

HepG2 cells were washed twice in EMEM (Bio Whittaker, USA) media supplemented with 200 μM L-glutamine (Bio Whittaker), 100U Penicillin, 100 μg streptomycin (Bio Whittaker), and 25 μM HEPES buffer; *N*-[2-hydroxyethyl]piperazine-*N*′-[2-ethanesulfonic acid] (Bio Whittaker). The cells were suspended at 2×10^5 cells mL^{-1} in EMEM Culture media (EMEM supplemented media, 10% foetal bovine serum (FBS); Bio Whittaker) then cells were left to adhere on polystyrene 6-well plates for 24 h in 37 °C, 5% CO_2, 95% humidity incubator. The cells were washed twice from debris and dead cells using EMEM supplemented media, then infected with 2% HCV-infected serum in EMEM culture medium with 8% FBS. Each of the tested compounds was added at concentrations of 10, 25, 50 and 100 μg mL^{-1}. Positive and negative control cultures were included. After 96 h incubation in 37 °C, 5% CO_2, 95% humidity incubator, another dose of the test compound was added. The cells were further incubated for another 96 h at 37 °C, 5% CO_2, 95% humidity, then the RNA was extracted. The positive strand and its replicating form (negative strand) of HCV were detected by RT-PCR using HCV specific primers to the 5′-untranslated region of the virus.

5.3.2. RNA extraction and RT-PCR of HCV RNA

Total RNA was extracted from HepG2 HCV-infected cells as well as from HepG2 HCV-infected cells that are treated with the test compounds using the method described in the literature [45]. Culture cells were mixed with 200 μL of 4 M guanidinium isothiocyanate containing 25 mM sodium citrate, 0.5% sarcosyl, 0.1 M β-mercaptoethanol and 100 μL sodium acetate. The lysed cells were mixed with an equal volume mixture of water-saturated phenol, chloroform and isoamyl alcohol. After vortexing of the sample, the mixture was centrifuged at 14K rpm for 10 min at 4 °C. The aqueous layer was collected and mixed with an equal volume of isopropanol. After incubation at −20 °C overnight, RNA was precipitated by centrifugation at 14K rpm for 30 min at 4 °C and the precipitated RNA was washed twice with 70% ethanol. The complimentary DNA (cDNA) and the first PCR reaction of the nested PCR detection system for the HCV RNA was performed in a 50 μL volume single-step reaction using the Ready-To-Go RT-PCR beads (Pharmacia Amersham Biotech, USA), 10 μM from each of the RT downstream primer, PCR forward primer and reverse primer P2. The thermal cycling protocol was manipulated as follows: 30 min at 42 °C for cDNA synthesis followed by 5 min at 95 °C and 30 cycles of 1 min at 94 °C, 1 min at 55 °C and 1 min at 72 °C. The nested PCR amplification was performed in 50 μL reaction mixture containing 0.2 mM from each dNTP, 10 μM from each of the reverse nested primer and the forward nested primer, two units of taq DNA polymerase (Promega, USA), 10 μL from the RT-PCR reaction in a 1X buffer supplied by Vendor. A fragment of 174 bp length was identified in positive samples.

References

[1] E. Aiello, S. Aiello, F. Mingoia, A. Bacchi, G. Pelizzi, C. Musiu, M.G. Setzu, A. Pani, P. La Colla, M.E. Marongiu, Bioorg. Med. Chem. 8 (2000) 2719–2728.

[2] M.S.A. El-Gaby, A.A. Atalla, A.M. Gaber, K.A. Abd Al-Wahab, Farmaco 55 (2000) 596–602.

[3] B.K. Kocyigit Kaymakcioglu, S. Rollas, Farmaco 57 (2002) 595–599.

[4] R. Storer, C.J. Ashton, A.D. Baxter, M.M. Hann, C.L.P. Marr, A.M. Mason, C.-L. Mo, P.L. Myers, S.A. Noble, H.R. Penn, N.G. Wier, G. Niall, J.M. Woods, P.L. Coe, Nucleosides Nucleotides 18 (2) (1999) 203–216.

[5] M.J. Genin, C. Biles, B.J. Keiser, S.M. Poppe, S.M. Swaney, W.G. Tarpley, Y. Yagi, D.L. Romero, J. Med. Chem. 43 (2000) 1034–1040.

[6] O. Moukha-chafiq, M.L. Taha, H.B. Lazrek, J.-J. Vasseur, C. Pannecouque, M. Witvrouw, E. De Clercq, Il Farmaco 57 (2002) 27–32.

[7] J. Ishida, H. Ohtsu, Y. Tachibana, Y. Nakanishi, K.F. Bastow, M. Nagai, H.-K. Wang, H. Itokawa, K.-H. Lee, Bioorg. Med. Chem. 10 (2002) 3481–3487.

[8] P.G. Baraldi, M.G. Pavani, M.d.C. Nunez, P. Brigidi, B. Vitali, R. Gambaric, R. Romagnolia, Bioorg. Med. Chem. 10 (2002) 449–456.

[9] S.A. Gamage, J.A. Spicer, G.W. Rewcastle, J. Milton, S. Sohal, W. Dangerfield, P. Mistry, N. Vicker, P.A. Charlton, W.A. Denny, J. Med. Chem. 45 (2002) 740–743.

[10] J. Goodchild, in: P.G. Sammes (Ed.), Topics in Antibiotic Chemistry, Ellis Horwood Limited–John Wiley and Sons, New York, 1982, p. 189.

[11] R.N. Comber, R.J. Gray, J.A. Secrist, Carbohydr. Res. 216 (1991) 441–452.

[12] A. Johansson, A. Poliakov, E.A. Kerblom, G. Lindeberg, S. Winiwarter, B. Samuelsson, U.H. Danielsonb, A. Hallberg, Bioorg. Med. Chem. (2002) 3915–3922.

[13] Salyers A.A., Whitt D.D. (Eds.), Microbiology Diversity, Disease and the Environment, Fitzgerald Science Press, Bethesda, Maryland, 2001, pp. 356.

[14] W.F. Goins, in: B.A. McClane, T.A. Mietzner (Eds.), Microbial Pathogenesis: A Principles-Oriented Approach, Fence Creek Publishing, Madison, 1999, p. 395.

[15] R. Bartenschlager, V. Lohmann, Antiviral Res. 52 (2001) 1–17.

[16] J. Aster, V. Kumar, in: R.S. Cotran, V. Kumar, T. Collins (Eds.), Pathologic Basis of Disease, W.B. Saunders Company, Philadelphia, 1999, pp. 860–861.

[17] N. Boyer, P. Marcellin, J. Hepatol. 32 (2000) 98–112.

[18] A.M. Farghaly, F.S.G. Soliman, M.M. El Semary, Sh.A.F. Rostom, Pharmazie 56 (2001) 28–32.

[19] Sh.A.F. Rostom, A.M. Farghaly, F.S.G. Soliman, M.M. El Semary, S. Elz, J. Lehmann, Arch. Pharm. Pharm. Med. Chem. 334 (2001) 241–247.

[20] H.T.Y. Fahmy, Sh.A.F. Rostom, A.A. Bekhit, Arch. Pharm. Pharm. Med. Chem. 335 (2002) 213–222.

[21] A.A. Bekhit, H.T.Y. Fahmy, Sh.A.F. Rostom, A. Baraka, Eur. J. Med. Chem. 38 (2003) 27–36.

[22] Bekhit A.A., Fahmy H.T.Y., Rostom Sh.A.F., Abdel-Aziem T., XXVIII International Conference of Pharmaceutical Sciences, Cairo, Egypt, 17–19 December 2002, Poster P-81.

[23] Silverman R.B. (Ed.), The Organic Chemistry of Drug Design and Drug Action, Academic Press, London, 1992, pp. 263.

[24] A.M. Al-Obaid, S.F. El-Shafie, M.S. Al-Mutairi, H.I. El-Subbagh, Sci. Pharm. 67 (1999) 129–147.

[25] I.H. Hall, N.J. Peaty, J.R. Henry, J. Easmon, G. Heinisch, G. Puerstinger, Arch. Pharm. Pharm. Med. Chem. 332 (1999) 115–123.

[26] S.E. Asis, A.M. Bruno, A.R. Martinez, M.V. Sevilla, C.H. Gaozza, A.M. Romano, J.D. Coussio, G. Ciccia, Farmaco 54 (1999) 517–523.

[27] S. Castellano, G. Stefancich, C. Musiu, P. La Colla, Arch. Pharm. Pharm. Med. Chem. 333 (2000) 299–304.

[28] S.G. Kucukguzel, S. Rollas, H. Erdeniz, M. Kiraz, A.C. Ekinci, A. Vidin, Eur. J. Med. Chem. 35 (2000) 761–771.

[29] G. Turan-Zitouni, Y. Blache, K. Gueven, Boll. Chim. Farmac. 140 (6) (2001) 397–400.

[30] H.T.Y. Fahmy, Boll. Chim. Farmac. 140 (6) (2001) 422–427.

[31] N. Demirbas, R. Ugurluoglu, A. Demirbas, Bioorg. Med. Chem. 10 (2002) 3717–3723.

[32] M. Kritsanida, A. Mouroutsou, P. Marakos, N. Pouli, S. Papakonstantinou-Garoufalias, C. Pannecouque, M. Witvrouw, E. De Clercq, Farmaco 57 (2002) 253–257.

[33] H.N. Dogan, A. Duran, S. Rollas, G. Sener, M.K. Uysal, D. Guelen, Bioorg. Med. Chem. 10 (2002) 2893–2898.

[34] M. Boiania, H. Cerecetto, M. Gonzalez, M. Risso, C. Olea-Azar, O.E. Piro, E.E. Castellano, A.L. de Cerain, O. Ezpeleta, A. Monge-Vega, Eur. J. Med. Chem. 36 (2001) 771–782.

[35] L.D.S. Yaday, S. Singh, Indian J. Chem. Sect. B 40 (2001) 440–442.

[36] G. Sahin, E. Palaska, M. Ekizoglu, M. Ozalp, Farmaco 57 (2002) 539–542.

[37] M.R. Grever, S.A. Schepartz, B.A. Chabner, Semin. Oncol. 19 (1992) 622–638.

[38] M.R. Boyd, K.D. Paull, Drug Rev. Res. 34 (1995) 91–109.

[39] A. Monks, D. Scudiero, P. Skehan, R. Shoemaker, K. Paull, D. Vistica, C. Hose, J. Jangley, P. Cronisie, A. Viagro-Wolff, M. Gray-Goodrich, H. Campell, M. Boyd, J. Natl. Cancer Inst. 83 (1991) 757–766.

[40] E.M. Acton, V.L. Narayanan, P.A. Risbood, R.H. Shoemaker, D.T. Vistica, M.R. Boyd, J. Med. Chem. 37 (1994) 2185–2189.

[41] H.I. El-Subbagh, W.A. El-Naggar, F.A. Badria, Med. Chem. Res. 3 (1994) 503–516.

[42] H.I. El-Subbagh, A.M. Al-Obaid, Eur. J. Med. Chem. 31 (1996) 1017–1021.

[43] A.H. Abadi, Arch. Pharm. Pharm. Med. Chem. 331 (1998) 352–358.

[44] N. Kato, M. Ikeda, T. Mizutani, K. Sugiyama, M. Noguchi, S. Hirohashi, K. Shimotohno, Jpn J. Cancer Res. 87 (1996) 787–792.

[45] M.K. El-Awady, S.M. Ismail, M. El-Sagheer, Y.A. Sabour, K.S. Amr, E.A. Zaki, Clin. Chim. Acta 283 (1999) 1–14.